

## *Candida albicans* cell wall comprises a branched $\beta$ -D-(1 $\rightarrow$ 6)-glucan with $\beta$ -D-(1 $\rightarrow$ 3)-side chains

Egidio Iorio,<sup>a,†</sup> Antonella Torosantucci,<sup>b,†</sup> Carla Bromuro,<sup>b</sup> Paola Chiani,<sup>b</sup>  
Amalia Ferretti,<sup>a</sup> Massimo Giannini,<sup>a</sup> Antonio Cassone<sup>b</sup> and Franca Podo<sup>a,\*</sup>

<sup>a</sup>Department of Cell Biology and Neurosciences, Istituto Superiore di Sanità, Viale Regina Elena, 299, Roma 00161, Italy

<sup>b</sup>Department of Infectious, Parasitic and Immune-mediated Diseases, Istituto Superiore di Sanità, Roma 00161, Italy

Received 4 October 2007; received in revised form 19 February 2008; accepted 23 February 2008

Available online 29 February 2008

**Abstract**—The structure of immunogenic and immunomodulatory cell wall glucans of *Candida albicans* is commonly interpreted in terms of a basic polysaccharide consisting of a  $\beta$ -D-(1 $\rightarrow$ 3)-linked glucopyranosyl backbone possessing  $\beta$ -D-(1 $\rightarrow$ 6)-linked side chains of varying distribution and length. This proposed molecular architecture has been re-evaluated by the present study on the products of selective enzymolysis of insoluble *C. albicans* glucan particles (GG). High resolution  $^1\text{H}$  (400 and 700 MHz) and  $^{13}\text{C}$  (100 and 175 MHz) NMR analyses were performed on a soluble  $\beta$ -glucan preparation (GG-Zym) obtained by GG digestion with endo- $\beta$ -D-(1 $\rightarrow$ 3)-glucanase and on its high- (Pool 1) and low-molecular weight (Pool 2) sub-fractions. The resonances typical of uniformly  $\beta$ -D-(1 $\rightarrow$ 6)- and  $\beta$ -D-(1 $\rightarrow$ 3)-linked linear glucans, together with additional multiplets assigned to short-chain oligoglucosides, were detected in GG-Zym. Pool 1 (46.3  $\pm$  6.4% of GG-Zym content) consisted of  $\beta$ -D-(1 $\rightarrow$ 6)-linked glucopyranosyl polymers, with short  $\beta$ -D-(1 $\rightarrow$ 3)-branched side chains of 2.20  $\pm$  0.02 units (branching degree (DB) = 0.14  $\pm$  0.03). Pool 2 was a mixture of glucose and linear short-chain  $\beta$ -D-(1 $\rightarrow$ 3)-oligoglucosides. Further digestion of Pool 1 by  $\beta$ -D-(1 $\rightarrow$ 6)-glucanase yielded a mixture of glucose and short  $\beta$ -D-(1 $\rightarrow$ 6)-linked, either linear or  $\beta$ -D-(1 $\rightarrow$ 3,6) branched, oligomers. These endoglucanase digestion patterns were consistent with the presence in *C. albicans* cell wall glucans of  $\beta$ -D-(1 $\rightarrow$ 6)-linked glucopyranosyl backbones possessing  $\beta$ -D-(1 $\rightarrow$ 3)-linked side chains, a structure very close to that of  $\beta$ -D-(1 $\rightarrow$ 6)-glucan from *Saccharomyces cerevisiae* yeast. This finding may provide the grounds for further elucidation of the cell wall structure and a better understanding of the biological properties of *C. albicans*  $\beta$ -glucans.

© 2008 Elsevier Ltd. All rights reserved.

**Keywords:** *Candida albicans*;  $\beta$ -Glucan; Endoglucanase; Branching degree; Fungal pathogen

### 1. Introduction

$\beta$ -Glucans are structurally complex, insoluble glucose homopolymers, found in the cell wall of fungi, algae and bacteria.<sup>1,2</sup> Their basic molecular structure is relatively homogeneous, although the type of bonding, molecular mass and overall molecular configuration may be variable depending on the microbial source.<sup>3</sup>

Biologically,  $\beta$ -glucans are well known for their immunomodulatory and antitumour properties.<sup>2,4,5</sup>

In the opportunistic fungal pathogen *Candida albicans*,  $\beta$ -glucans are major structural components, accounting for approximately 50–60% of cell wall dry weight.<sup>6</sup> Based on different solubility in alkali and acid, *C. albicans*  $\beta$ -glucan has been differentiated into an alkali-soluble polymer of a relatively low molecular weight and a branched, acid-soluble molecule, both predominantly composed of  $\beta$ -D-(1 $\rightarrow$ 6)-linked residues, plus an alkali-acid insoluble, highly branched complex, containing grossly equivalent amounts of  $\beta$ -D-(1 $\rightarrow$ 6) and  $\beta$ -D-(1 $\rightarrow$ 3) linkages in a complex with chitin.<sup>7</sup> When optimally preserved, this  $\beta$ -glucan-chitin complex reveals a

\* Corresponding author. Tel.: +39 0649902686; fax: +39 0649387144; e-mail: [franca.podo@iss.it](mailto:franca.podo@iss.it)

<sup>†</sup> These authors contributed equally to the study.

highly interwoven fibrillar constitution and retains the shape of the cell of origin, indicating its prominent role in providing form and structural integrity to the fungal wall.<sup>7</sup>

Models of cell wall structure suggest that the  $\beta$ -D-(1 $\rightarrow$ 3)-linked glucan molecules form a three-dimensional matrix surrounding the fungal cell. At the inside, close to the plasma membrane, this skeletal framework is strengthened by chitin chains, whereas, at its outer edge,  $\beta$ -D-(1 $\rightarrow$ 6) glucan moieties link GPI-anchored cell wall mannoproteins to the skeletal framework.<sup>8</sup> According to the prevailing view, the basic structure of *C. albicans*  $\beta$ -glucans is proposed to consist of  $\beta$ -D-(1 $\rightarrow$ 3)-linked glucopyranosyl backbones possessing  $\beta$ -D-(1 $\rightarrow$ 6)-linked side chains of varying distribution and length, whose degree of branching (DB) is reputed to be related to the immunomodulatory properties of these glucans.<sup>9,10</sup>

Besides evidence on their antitumour and immunoadjuvant properties, the view has progressively emerged that cell wall  $\beta$ -glucans may also represent an important target for pharmacological or immunotherapeutic interventions in the treatment of fungal infections.<sup>11–15</sup>  $\beta$ -Glucan synthesis is a crucial event for fungal growth and virulence, and its blockade is the common mechanism of action of novel candidacidal agents, such as caspofungin and micafungin.<sup>13</sup> Moreover, polyclonal or monoclonal antibodies and peptides thereof targeting  $\beta$ -glucans have been shown to cause a marked candidacidal effect in vitro and to confer a significant protection against experimental mucosal or disseminated candidiasis.<sup>12,14,15</sup> Due to their weak intrinsic immunogenicity,<sup>15–17</sup> *C. albicans*  $\beta$ -glucans have received very little attention as fungal antigens. Nonetheless, specific humoral responses directed against these  $\beta$ -glucans can be generated in animal models upon suitable immunization conditions.<sup>12,15,17</sup> These responses may confer a remarkable anti-*Candida* protection, opening the way to a potential use of  $\beta$ -glucan conjugates as vaccines.<sup>12</sup>

While adding  $\beta$ -glucans to the list of the few potentially protective fungal antigens so far described, the overall body of novel biological findings calls for a well-established characterization of the molecular structure of these compounds and of their organization in the *C. albicans* cell wall.

To this end, we undertook a molecular characterization of  $\beta$ -glucans obtained from the digestion of pure, insoluble glucan particles by selective endo-glucanases. One- (1D) and two-dimensional (2D) nuclear magnetic resonance (NMR) techniques at high or very high field were employed throughout this investigation because of their recognized capability of disclosing primary structure, DB, degree of polymerization (DP) and configuration of oligo- and polysaccharide chains.<sup>1,18–20</sup>

## 2. Results

### 2.1. Identification of $\beta$ -D-(1 $\rightarrow$ 6)- and $\beta$ -D-(1 $\rightarrow$ 3)-linked glucopyranosyl units in GG-Zym

A particulate preparation of alkali-acid insoluble *C. albicans* glucan (GG), practically devoid of mannoprotein or protein contaminants,<sup>21</sup> was digested by  $\beta$ -D-(1 $\rightarrow$ 3)-glucanase to yield the soluble  $\beta$ -glucan fraction named GG-Zym (see Section 4). Typically, digestion of 10 mg of GG yielded approximately 5 mg of GG-Zym (estimated by assay of carbohydrate content against a glucose standard).

A representative <sup>1</sup>H 1D NMR spectrum (700 MHz, 25 °C), obtained from GG-Zym in D<sub>2</sub>O, is compared

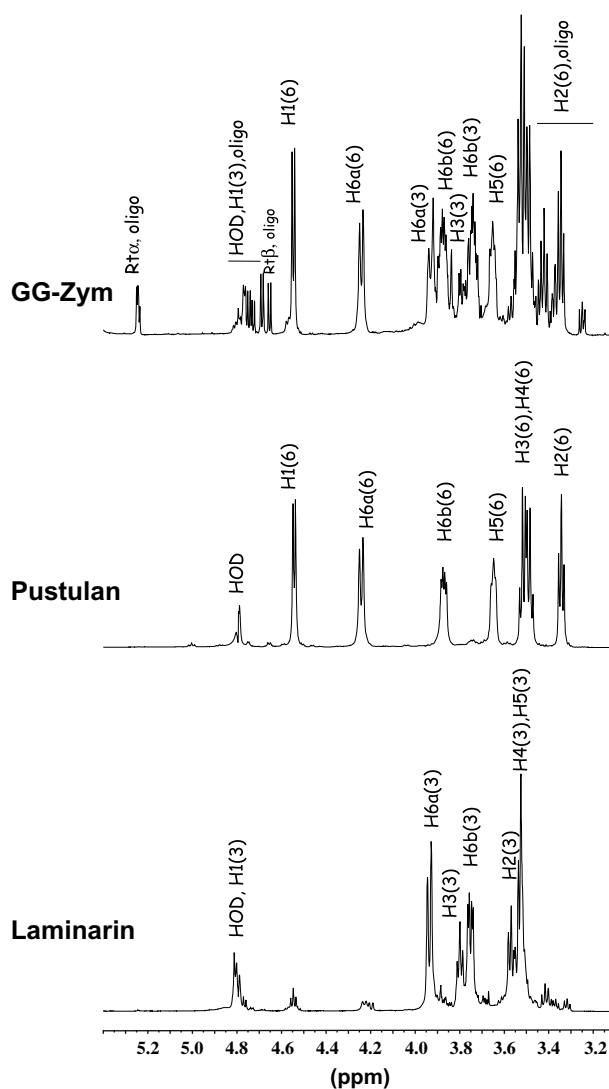


**Figure 1.** Representative <sup>1</sup>H NMR spectra (700 MHz) of GG-Zym and two linear long chain  $\beta$ -D-(1 $\rightarrow$ 6)- and  $\beta$ -D-(1 $\rightarrow$ 3)-linked standards, pustulan and laminarin (D<sub>2</sub>O, 25 °C). Signals arising from  $\beta$ -D-(1 $\rightarrow$ 6) and  $\beta$ -D-(1 $\rightarrow$ 3)-linked glucopyranosyl units are, respectively, indicated by (6) and (3), while resonances due to short glucopyranosyl chains are indicated as 'oligo'.

in Figure 1 with those of two standard long-chain homopolymers of  $\beta$ -D-(1 $\rightarrow$ 6)- and  $\beta$ -D-(1 $\rightarrow$ 3)-linked glucopyranosyl units, pustulan and laminarin, respectively. These spectra allowed direct identification in GG-Zym of all major (either distinct or partially overlapping) resonances typical of uniformly  $\beta$ -D-(1 $\rightarrow$ 6)- or  $\beta$ -D-(1 $\rightarrow$ 3)-linked linear glucans.<sup>22–24</sup> Distinct signals were in particular detected in GG-Zym for pustulan-like chemical groups, such as H1(6) (the proton in position 1 of  $\beta$ -D-(1 $\rightarrow$ 6)-linked units, doublet centred at  $\delta$  4.55); H6a(6) ( $\delta$  4.24); H6b(6) ( $\delta$  3.88) and H5(6) ( $\delta$  3.65). Resonances typical of  $\beta$ -D-(1 $\rightarrow$ 3)-linked units, such as H6a(3), H3(3) and H6b(3), were also easily identified at  $\delta$  3.93, 3.76 and 3.74, respectively. However, even at this very high field, other  $^1\text{H}$  NMR signals from either  $\beta$ -D-(1 $\rightarrow$ 6)- or  $\beta$ -D-(1 $\rightarrow$ 3)-linked units were grouped together under complex resonance profiles, such as H2(3), H4(3), H5(3), H3(6) and H4(6) signals, all appearing around  $\delta$  3.52, and H2(6) ( $\delta$  3.34), which overlapped with a series of additional multiplets not present in the spectra of long-chain homopolymers. These additional multiplets were attributed to short-chain oligoglucoside sequences (indicated as ‘oligo’ in the spectra). Primary support for this assignment was the detection in GG-Zym spectra of the typical signals of terminal reducing ends (RT), either in  $\alpha$  or  $\beta$  anomeric conformations (two close RT $\alpha$  doublets at  $\delta$  5.24 and two distinct RT $\beta$  doublets at 4.65 and 4.69), whose relatively high intensity clearly indicated the presence of substantial amounts of short oligoglucosides in the GG-Zym preparation.<sup>23–26</sup>

Two-dimensional heteronuclear ( $^1\text{H}$ -decoupled  $^{13}\text{C}$ - $^1\text{H}$  HSQC) and homonuclear ( $^1\text{H}$ - $^1\text{H}$  COSY) sequences allowed the assignment of all  $^1\text{H}$  and  $^{13}\text{C}$  resonances detected in GG-Zym and in reference compounds, on the basis of  $^{13}\text{C}/^1\text{H}$  and  $^1\text{H}/^1\text{H}$  cross-peaks (Fig. 2 and Table 1). Furthermore, double resonance HSQC-DEPT experiments (not shown) confirmed unambiguous identification of the  $^{13}\text{C}$  resonances arising

**Table 1.** Assignment of  $^{13}\text{C}/^1\text{H}$  NMR cross-peaks (175 MHz/700 MHz) to  $\beta$ -D-(1 $\rightarrow$ 3)- and  $\beta$ -D-(1 $\rightarrow$ 6)-linked glucopyranosyl units in HSQC ( $\text{D}_2\text{O}$ , 25 °C) analyses of GG-Zym, pustulan and laminarin ( $\delta$ , ppm)

<sup>13</sup> C/H	Pustulan	Laminarin	GG-Zym	
			β-D-(1→6)	β-D-(1→3)
<i>Backbone</i>				
C1/H1	104.14/4.54	103.99/4.80	104.23/4.55	103.99/4.75
C2/H2	74.25/3.35	74.67/3.57	74.45/3.34	74.39/3.55
C3/H3	76.87/3.51	85.63/3.80	76.94/3.50	85.94/3.76
C4/H4	70.70/3.49	69.42/3.53	70.68/3.48	69.15/3.52
C5/H5	75.96/3.65	77.03/3.52	76.03/3.65	75.11/3.43
C6/H6a	70.04/4.24	61.90/3.93	70.10/4.24	61.97/3.93
C6/H6b	70.04/3.87	61.90/3.75	70.06/3.87	61.90/3.74
<i>Reducing ends</i>				
C1/H1(RTα)	bd	bd	93.43/5.24 <sup>a</sup>	
C1/H1(RTβ)	bd	bd	97.13/4.68; 97.33/4.65	
C3/H3(RTα)	bd	bd	83.80/3.92	
C3/H3(RTβ)	bd	bd	85.75/3.79	

bd: Below detection.

<sup>a</sup> Two unresolved doublets.

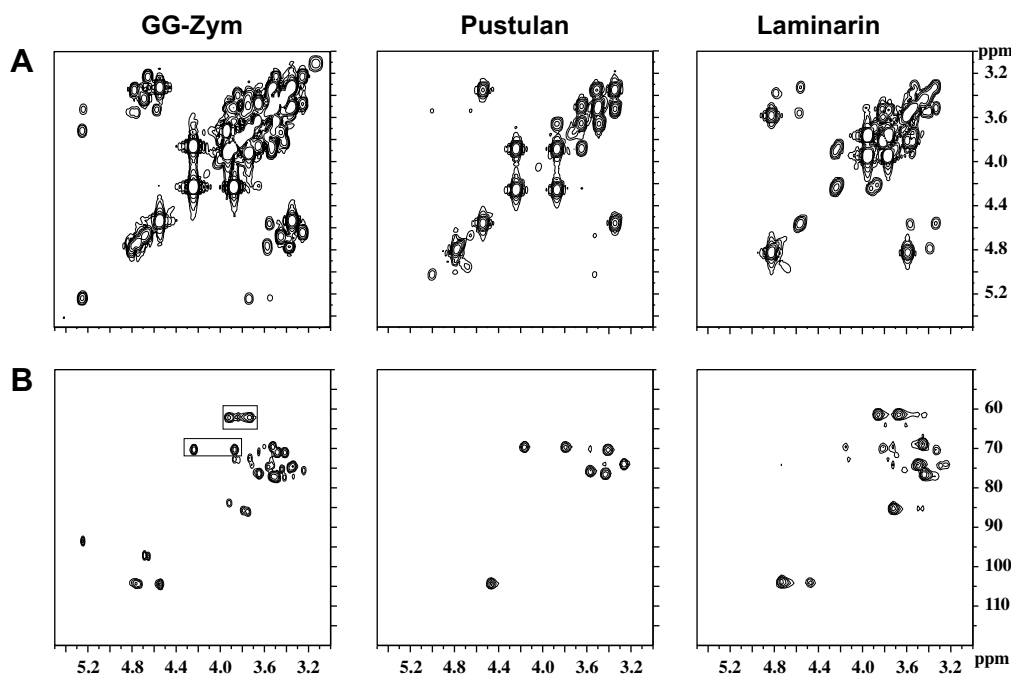


**Figure 2.** 2D NMR spectra of GG-Zym and two long chain  $\beta$ -D-(1 $\rightarrow$ 6)- and  $\beta$ -D-(1 $\rightarrow$ 3)-linked standards, pustulan and laminarin ( $\text{D}_2\text{O}$ , 25 °C). A,  $^1\text{H}$ - $^1\text{H}$  magnitude correlation spectroscopy (COSY, 700 MHz); B,  $^1\text{H}$ - $^{13}\text{C}$  heteronuclear single quantum correlation spectroscopy (HSQC, 700 MHz/175 MHz).

ing from C6 of either  $\beta$ -D-(1 $\rightarrow$ 6)- or  $\beta$ -D-(1 $\rightarrow$ 3)-linked glucopyranosyl residues (indicated in boxes in Fig. 2), on the basis of selective signal inversion due to  $^{13}\text{C}$ -coupling to the respective pair of covalently bound protons (C6/H6a and C6/H6b).<sup>27</sup> The overall analysis of these 2D maps confirmed the identification in GG-Zym of the major cross-peaks typical of  $\beta$ -D-(1 $\rightarrow$ 6)- and  $\beta$ -D-(1 $\rightarrow$ 3)-linked glucopyranosyl units, in general agreement with previous reports on glucans isolated from the cell wall of a variety of yeast, seaweed, lichen and fungal species, including *C. albicans*.<sup>26,28–35</sup> Moreover, with respect to 1D spectra, 2D maps allowed clearer discrimination of signals due to reducing ends from those of other residues of oligoglucosides (Table 1).

## 2.2. Composition of the GG-Zym chromatographic sub-fractions (Pool 1 and Pool 2)

The NMR analyses described above suggested the co-existence of long- and short-chain components in the GG-Zym preparation. Accordingly, separation of this material by gel filtration chromatography through a Bio-Gel P2 resin (see Experimental) yielded two major fractions, Pool 1 (eluted in column void volume) and Pool 2, comprising molecular masses below 1800 dalton (data not shown). Mean percent yield  $\pm$  SD of the two fractions, with respect to the total amount of GG-Zym loaded on the column, was  $46.3 \pm 6.4\%$  for Pool 1 and  $39.1 \pm 2.0\%$  for Pool 2, in four independent preparations.

Further gel-filtration analysis to estimate molecular mass of Pool 1 component(s), revealed a major polysaccharide peak, co-eluting with pustulan (20,000 dalton) and representing approximately 50% of the total Pool 1 material, and a series of polydisperse polysaccharide molecules of lower apparent molecular masses (18,500 to 16,000 dalton). In turn, Pool 2 apparently consisted of a family of short oligosaccharides with DP ranging from 3 to 5. Triose molecules were predominant, accounting for 43% of the total carbohydrate eluted from the column. Pool 2 fraction also contained an appreciable (about 25%) amount of monosaccharide (data not shown).

NMR analysis was carried out on Pool 1 and Pool 2 fractions dissolved in  $\text{Me}_2\text{SO}-d_6$ - $\text{D}_2\text{O}$  6:1, at 80 °C. The use of these experimental conditions allowed the advantages of (a) preventing molecular aggregation; (b) achieving a better spectral resolution; and (c) removing the residual HDO signal from the region typical of anomeric protons.<sup>28</sup> As a result, a better separation of peaks due to H1 protons, respectively belonging to reducing terminals (RT), to the second unit next to a reducing terminal (SRT), to non-reducing terminals (NRT), as well as to backbone (BC) and side chain (SC) residues was obtained.<sup>28,35</sup>

Partial  $^1\text{H}$  NMR spectra ( $\delta$  4.30–5.20) of GG-Zym, Pool 1 and Pool 2 in  $\text{Me}_2\text{SO}-d_6$ - $\text{D}_2\text{O}$  are compared in Figure 3 with those of pustulan, laminarin and linear short-chain  $\beta$ -D-(1 $\rightarrow$ 3)-linked oligoglucosides of increasing length ( $L_n$ ) and free glucose (G). Peak assignments are indicated on the respective spectral profiles. The rigid downfield shift of the Pool 2 spectrum was attributed to small differences in diamagnetic susceptibility and ionic strength of this sample. The H1(6) protons of the backbone pustulan chain (BC(6)) gave a doublet at  $\delta$  4.34, while the H1(3) protons of the laminarin backbone (BC(3)) gave a doublet at  $\delta$  4.60. Although mainly composed of linear  $\beta$ -D-(1 $\rightarrow$ 3)-linked glucopyranosyl units, laminarin clearly possessed a small fraction of short  $\beta$ -D-(1 $\rightarrow$ 6)-side segments, as demonstrated by a minor doublet at  $\delta$  4.31, typical of terminal (TSC(6)) units.<sup>28</sup> The DB of laminarin determined from the relative TSC(6) peak area was about 0.07, in general agreement with DB values typically reported for laminarins from different sources.<sup>23,24,36</sup> Pool 2 clearly represented a mixture of short-chain  $L_n$  and free glucose, in agreement with chromatographic analysis. A more detailed characterization of Pool 2 and Pool 1 is reported below.

## 2.3. Oligosaccharide composition of Pool 2

Comparison of the Pool 2 spectral profile in  $\text{Me}_2\text{SO}-d_6$ - $\text{D}_2\text{O}$  with those of glucose and  $L_n$  oligomers of increasing chain length (Fig. 3) allowed identification in this glucan subfraction of free glucose from the doublets of its anomeric forms at  $\delta$  4.97 ppm (GRT $\alpha$ ) and  $\delta$  4.35 (GRT $\beta$ ), while the signals of reducing ends of  $L_n$  oligosaccharides appeared at lower fields (RT $\alpha$  at  $\delta$  5.03 and RT $\beta$  at  $\delta$  4.44, respectively). The spectra of laminaritriose (L3) and laminaritetraose (L4) showed an additional doublet arising from H1 of the NRT unit (which exhibited identical chemical shift in both oligomers), whereas the doublet of H1 due to internal backbone (BC) units only appeared at  $\delta$  4.57 for oligomers equal or longer than 4 units ( $L_n$  ( $n \geq 4$ )), in agreement with the spectra reported for laminaripentaose (L5) and laminariheptaose (L7) by Kim et al.<sup>28</sup> No other peaks, attributable to either branched or linear  $\beta$ -D-(1 $\rightarrow$ 6)-linked oligomers were detected. The average length ( $l$ ) of  $L_n$  oligosaccharides present in Pool 2, calculated as the ratio between the total area ( $a$ ) of all H1 peaks (excluding GRT $\alpha$  and GRT $\beta$ ) and the area of RT anomers ( $l(L_n) = a(\text{all H1})/[a(\text{RT}\alpha) + a(\text{RT}\beta)]$ ) was  $2.6 \pm 0.2$  units.

Moreover, the doublet due to H1 of BC(3) was only barely detectable in Pool 2, indicating that this subfraction comprised only a very low amount of linear  $\beta$ -D-(1 $\rightarrow$ 3)-linked oligomers equal or longer than 4 units. In fact, the average length of these oligosaccharides ( $l(L_n(n \geq 4)) = 3 + a(\text{H1(BC)})/[a(\text{RT}\alpha) + a(\text{RT}\beta)]$ ) was  $4.1 \pm 0.1$ .



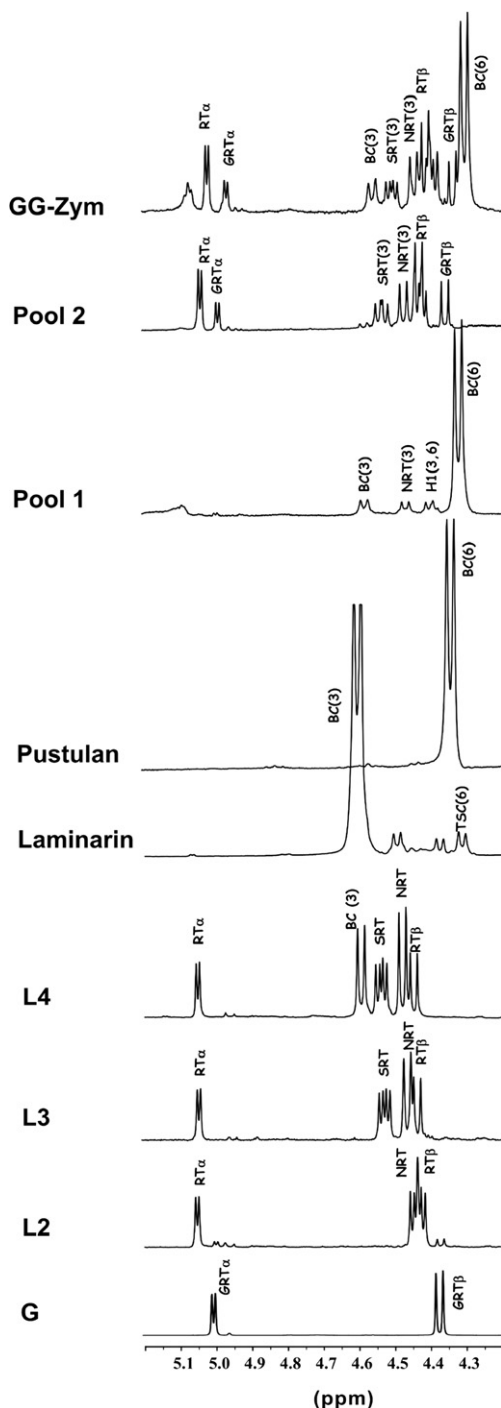


**Figure 3.**  $^1\text{H}$  NMR spectra (400 MHz) of GG-Zym and its subfractions Pool 1 and Pool 2 in  $\text{Me}_2\text{SO}-d_6\text{-D}_2\text{O}$  6:1 (80 °C), as compared to the spectral profiles of the two linear long chain  $\beta\text{-D-(1}\rightarrow\text{6)}$ - and  $\beta\text{-D-(1}\rightarrow\text{3)}$ -linked standards pustulan and laminarin, short  $\beta\text{-D-(1}\rightarrow\text{3)}$ - $\beta$ -linked oligoglucosides laminaribiose (L2), laminaritriose (L3) and laminaritetraose (L4) and free glucose (G). Signals of H1 protons in  $\beta\text{-D-(1}\rightarrow\text{6)}$ - and  $\beta\text{-D-(1}\rightarrow\text{3)}$ -linked chains are, respectively, indicated by (6) and (3). H1 protons at the branch-point between  $\beta\text{-D-(1}\rightarrow\text{6)}$ - and  $\beta\text{-D-(1}\rightarrow\text{3)}$ -linked chains are indicated by H1(3,6). H1 protons belonging to reducing terminals (RT), to the second unit next to a reducing terminal (SRT), to non-reducing terminal (NRT) and backbone (BC) are indicated on the spectra. In the spectrum of laminarin, TSC(6) denotes the H1 proton of the single or terminal glucopyranosyl unit in the  $\beta\text{-D-(1}\rightarrow\text{6)}$  side chain (see also Ref. 28).

We could therefore exclude the presence in Pool 2 of any substantial amount of long laminarin-like chains (as expected from effective  $\beta\text{-D-(1}\rightarrow\text{3)}$ -endoglucanase digestion). Furthermore, the presence in Pool 2 of  $\beta\text{-D-(1}\rightarrow\text{6)}$ -branched  $\beta\text{-D-(1}\rightarrow\text{3)}$ -oligomers could also be ruled out, because the corresponding side chains would give rise to the typical doublet of TSC(6) units, which was not detected in Pool 2 spectra.

In conclusion, the Pool 2 fraction essentially comprised short  $L_n$  oligosaccharides with an average DP of 2.6 units, and free glucose.

#### 2.4. Structure of Pool 1 polysaccharides

Pool 1 mainly comprised  $\beta\text{-D-(1}\rightarrow\text{6)}$ -linked glucopyranosyl chains, since its spectrum in  $\text{Me}_2\text{SO}-d_6\text{-D}_2\text{O}$  at 80 °C practically coincided with that of pustulan, not only in the reported spectral region (Fig. 3), but also in the overall frequency range (not shown), with the exception of a few additional minor peaks. In particular, the small doublets centred at  $\delta$  4.58 and 4.52, respectively coincident with those of H1 in BC(3) and non-reducing terminal NRT(3) units in short-chain  $L_n$  oligomers, were attributed to inner and terminal  $\beta\text{-D-(1}\rightarrow\text{3)}$ -linked side chains of  $\beta\text{-D-(1}\rightarrow\text{6)}$ -linked backbones. Moreover, the doublet at  $\delta$  4.41 in Pool 1 spectra was tentatively assigned to  $\beta\text{-D-(1}\rightarrow\text{3,6)}$ -linked units in the  $\beta\text{-D-(1}\rightarrow\text{6)}$  chain. The H1 proton of this branch point unit is also most likely responsible for the minor doublet at about  $\delta$  4.56, detected at the foot of the H1(6) doublet ( $\delta$  4.55) in the spectrum of GG-Zym in  $\text{D}_2\text{O}$  (see Fig. 1 and Ref. 32). The branch-point H1 resonance is, in fact, expected to be slightly downfield shifted with respect to the H1 protons of BC(6) units, in agreement with the previous peak assignment to analogous sequences.<sup>23,26</sup> Peak area quantification of H1 signals (in  $\text{Me}_2\text{SO}-d_6\text{-D}_2\text{O}$  at 80 °C) showed that the average Pool 1 branching degree ( $\text{DB} = a[\text{NRT(3)}]/a[\text{H1(6)}]$ ) was  $0.14 \pm 0.03$  (i.e., one side chain every seven  $\beta\text{-D-(1}\rightarrow\text{6)}$ -linked units) with an average  $\beta\text{-D-(1}\rightarrow\text{3)}$  side chain length  $l(\text{SC(3)}) = 1 + a[\text{BC(3)}]/a[\text{NRT(3)}] = 2.20 \pm 0.02$  units, including the non-reducing end, but excluding the branch point unit.

#### 2.5. Composition of $\beta\text{-(1}\rightarrow\text{6)}$ -glucanase digestion products of Pool 1

To further confirm the presence of  $\beta\text{-D-(1}\rightarrow\text{3,6)}$  branching in the structure of Pool 1 polysaccharides, this GG-Zym subfraction was further digested by endo- $\beta\text{-D-(1}\rightarrow\text{6)}$ -glucanase. Figure 4 reports typical  $^1\text{H}$  NMR spectra of  $\beta\text{-D-(1}\rightarrow\text{6)}$ -glucanase-mediated digestion products of Pool 1, as compared to those of pustulan, of linear  $\beta\text{-D-(1}\rightarrow\text{6)}$ -linked oligomers such as gentiobiose (G2), gentiotriose (G3) and free glucose, dissolved in  $\text{Me}_2\text{SO}-d_6\text{-D}_2\text{O}$  6:1 (80 °C). The G2 spectral profile

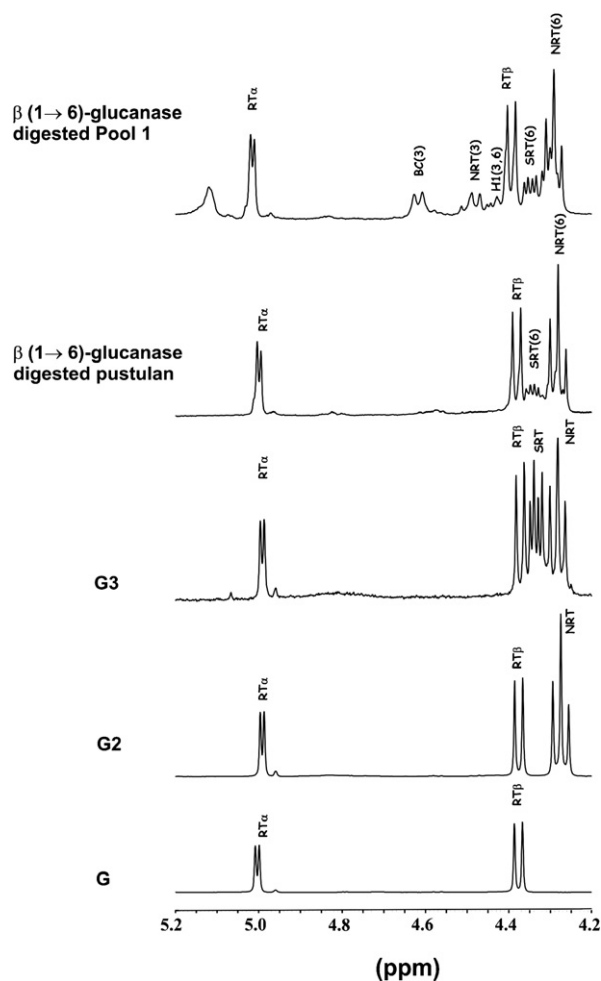


**Figure 4.**  $^1\text{H}$  NMR spectra (400 MHz) of Pool 1 and pustulan  $\beta$ -D-(1 $\rightarrow$ 6)-glucanase digest products, as compared to glucose (G), gentiobiose (G2) and gentiotriose (G3) in  $\text{Me}_2\text{SO}-d_6$ - $\text{D}_2\text{O}$  6:1 (80  $^\circ\text{C}$ ). H1 protons belonging to reducing terminals (RT), to the second unit next to a reducing terminal (SRT), to non-reducing terminal (NRT), backbone (BC) are indicated.

was in accordance with that reported by Kim et al.,<sup>28</sup> under the same solvent and temperature conditions. Quantitative spectral analyses showed that (a) the typical H1 signals arising from branched  $\beta$ -D-(1 $\rightarrow$ 3) side chains in Pool 1 (peaks BC(3), NRT(3) and H1(3,6) in Fig. 3) were practically maintained unaltered following digestion of this glucan fraction by endo- $\beta$ -D-(1 $\rightarrow$ 6)-glucanase; and (b) these peaks were not detected in the mixture of pustulan digestion products, in which the original BC(6) peak practically disappeared in favour of short linear  $\beta$ -D-(1 $\rightarrow$ 6)-linked oligomers (Gn) and free glucose. The percentage of free glucose determined by the relationship  $[a(\text{RT}\alpha) + a(\text{RT}\beta)] - a[\text{NRT}(6)] / [a(\text{RT}\alpha) + a(\text{RT}\beta)] \times 100$  was about 2% in Pool 1 digest and 7% in pustulan digest, indicating that the presence of (1 $\rightarrow$ 3,6)-linked units in the former reduced the efficiency of digestion of the Pool 1 polysaccharide backbone to some extent. Comparison of the

overall digestion patterns of Pool 1 and pustulan was made possible by the quantification of the multiplet centred at  $\delta$  4.33, due to SRT(6) (i.e., the unit adjacent to the reducing end of G3 or longer Gn oligomers), which allowed the determination of the percentage of  $\beta$ -D-(1 $\rightarrow$ 6)-oligomers with  $n \geq 3$  in Pool 1 and in pustulan digestion mixtures. All together, these analyses showed that the concentration ratios of G:G2:Gn ( $n \geq 3$ ) were 2:64:34 in Pool 1 and 7:61:32 in pustulan. The spectrum of Pool 1 digest qualitatively differed from that of pustulan for the presence of two (instead of only one), partially overlapping NRT(6) multiplets. The additional, downfield shifted multiplet was attributed to the presence in Pool 1 digest of Gn oligomers with non-reducing terminal units adjacent to (1 $\rightarrow$ 3,6)-branch points (see also Ref. 26).

Finally, the peak area ratio of NRT(3) to the overall NRT(6) profile was about 0.13, indicating that about 13% of Pool 1-derived oligomers had a 3-branched side chain.

## 2.6. NMR cross-peaks are fingerprints of the overall GG-Zym composition in water

Collectively, NMR analyses on glucan preparations in  $\text{Me}_2\text{SO}-\text{D}_2\text{O}$  (Figs. 3 and 4) showed that GG-Zym comprised a combination of long  $\beta$ -D-(1 $\rightarrow$ 6) backbones possessing short  $\beta$ -D-(1 $\rightarrow$ 3) side chains (Pool 1) and short Ln oligosaccharides (Pool 2).

It is interesting to note the capability of 2D COSY maps to give a direct, straightforward identification of the main GG-Zym components in  $\text{D}_2\text{O}$ , by using H1/H2 cross-peaks as fingerprints of structural identification, even without physical chromatographic separation of GG-Zym in Pool 1 and Pool 2 fractions (Fig. 5). In fact, the 5.24/3.54 and 4.66/3.25 cross-peaks reflect the content of free glucose anomers; the RT units of  $\beta$ -D-(1 $\rightarrow$ 3)-linked oligosaccharides in Pool 2 give distinct cross-peaks at  $\delta$  5.25/3.74 (RT $\alpha$ ) and  $\delta$  4.69/3.45 (RT $\beta$ ), while the corresponding NRT unit resonates at  $\delta$  4.78/3.37 and the spectral contributions of internal glucopyranosyl residues of  $\beta$ -D-(1 $\rightarrow$ 3) oligoglucosides (BC(3) and SRT(3)) merge together at  $\delta$  4.78/3.57. Regarding Pool 1 components, two well-separated peaks are detected at  $\delta$  4.56/3.35 and 4.57/3.55, respectively, due to H1 of long  $\beta$ -D-(1 $\rightarrow$ 6)-linked backbones (BC(6)) and to their 3-substituted glucopyranosyl residues serving as branching points to  $\beta$ -D-(1 $\rightarrow$ 3) side chains. On the other hand, the contributions of H1 protons on BC(3) and NRT(3) units of these side chains overlap with cross-peaks arising from the Ln oligosaccharides present in Pool 2. The identification of these cross-peaks as fingerprints of GG-Zym composition may be useful for future analysis of *C. albicans* glucan preparations obtained by different procedures.

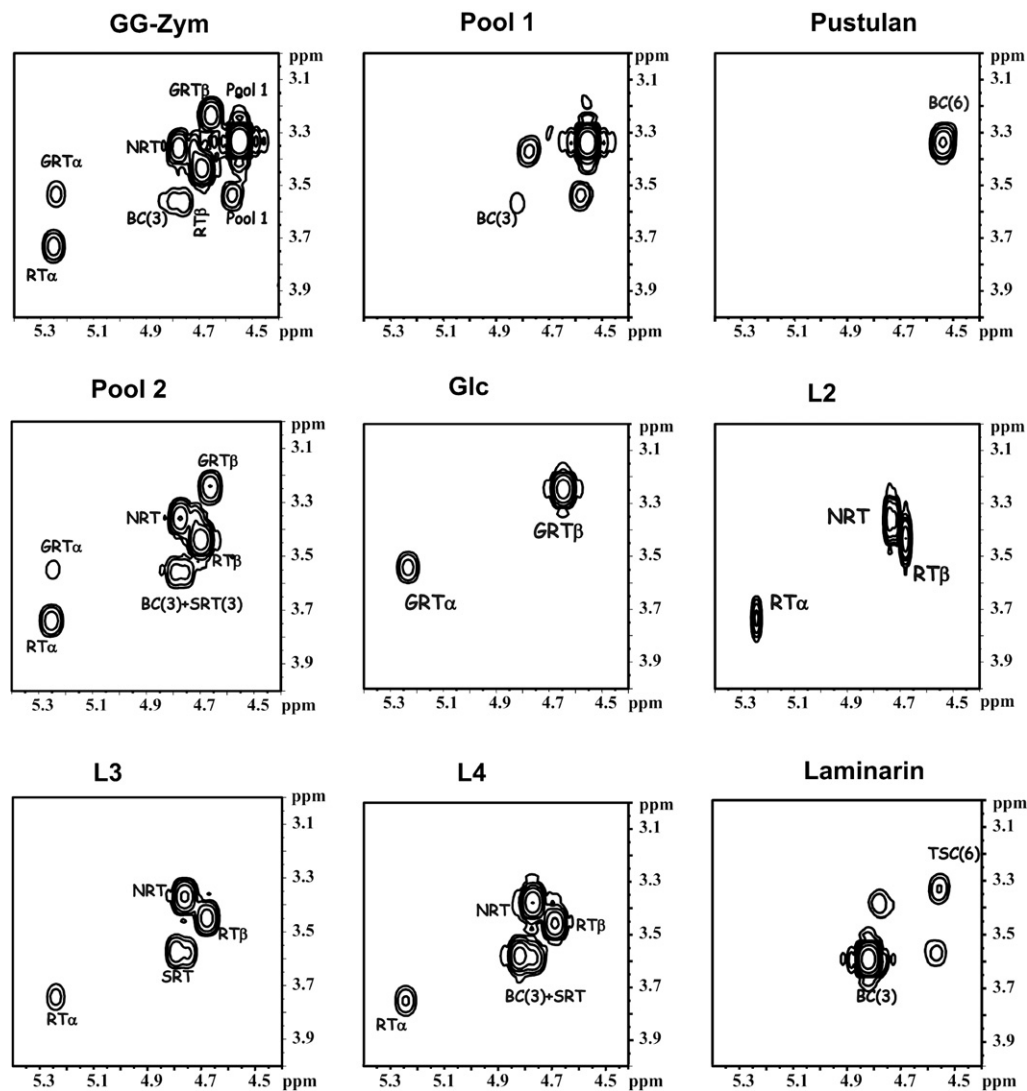


**Figure 5.** Identification of cross-peaks as ‘fingerprints’ of  $\beta$ -D-(1 $\rightarrow$ 3)- and  $\beta$ -D-(1 $\rightarrow$ 6)-linked components in 2D COSY  $^1\text{H}$  NMR maps (700 MHz) of GG-Zym, its fractions Pool 1 and Pool 2 and reference compounds (pustulan, laminarin and *Ln* oligosaccharides) in  $\text{D}_2\text{O}$  (25  $^\circ\text{C}$ ).

### 3. Discussion

Chitin-interconnected, alkali-acid-insoluble  $\beta$ -glucans form the skeletal framework of the fungal cell wall, and their degradation, or any inhibition of or interference with their synthesis, rapidly leads to the arrest of fungal growth and to cellular death by lysis.<sup>7,11,37</sup>

Unequivocal determination of the natural organization of  $\beta$ -glucans in *C. albicans* cell wall appears essential to identify molecular mechanisms of pharmacological or immunological targeting of this cell wall component for the prevention and treatment of infections by this and other opportunistic fungi.<sup>5,7,11,12,14,15,37,38</sup> Elucidation of  $\beta$ -glucans architecture is also on the basis of a better understanding of the relationships between structural parameters and immunostimulating activities of these compounds in vitro and in vivo.<sup>34,39–43</sup>

The most generally accepted model proposes a basic structure of *C. albicans*  $\beta$ -glucans in terms of  $\beta$ -D-(1 $\rightarrow$ 3)-linked backbones holding  $\beta$ -D-(1 $\rightarrow$ 6)-linked side chains of varying distribution and length.<sup>9,10</sup> The degree of  $\beta$ -D-(1 $\rightarrow$ 3,6)-branching on the  $\beta$ -D-(1 $\rightarrow$ 3)-chains is reputed to correlate with the overall  $\beta$ -glucan biological properties. A similar condition has also been reported for  $\beta$ -glucans isolated from a variety of mushrooms, in which the content of  $\beta$ -D-(1 $\rightarrow$ 6)-side chains (typically one every 2–3 units in  $\beta$ -(1 $\rightarrow$ 3)-backbones) was found to correlate with antitumour activity.<sup>44–47</sup>

There are still, however, uncertainties on the fine structure of  $\beta$ -glucans in their natural arrangement in *C. albicans*, because the harsh protocols commonly adopted for  $\beta$ -glucans solubilization in alkali or acid media may degrade the native structure of these polysaccharides to variable extents. Different levels of  $\beta$ -D-(1 $\rightarrow$ 3)- and  $\beta$ -D-(1 $\rightarrow$ 6)-linked chains (with no mixed

intra-chain  $\beta$ -D-(1 $\rightarrow$ 3)/ $\beta$ -D-(1 $\rightarrow$ 6) linkages) and polymers with variable degrees of branching have therefore been reported according to the different conditions adopted for  $\beta$ -glucan preparation.<sup>29,34,35</sup>

A powerful approach for a mild and controlled solubilization of fungal  $\beta$ -glucans is offered by the use of selective, purified hydrolytic enzymes, such as  $\beta$ -D-(1 $\rightarrow$ 3)- and  $\beta$ -D-(1 $\rightarrow$ 6)-glucanases.<sup>6,26,48–50</sup> In the present work, we first applied a mild treatment with endo- $\beta$ -D-(1 $\rightarrow$ 3)-glucanase, to selectively digest highly purified, mannan- and protein-free, alkali-acid-insoluble  $\beta$ -glucan ghosts (GG).<sup>21</sup>

### 3.1. Structure of a 3-branched $\beta$ -D-(1 $\rightarrow$ 6)-glucan component from *C. albicans* cell wall

NMR analyses on the endo- $\beta$ -D-(1 $\rightarrow$ 3)-glucanase GG digest (GG-Zym) and on its high MW chromatographic fraction (Pool 1) allowed us to identify a previously unreported  $\beta$ -D-(1 $\rightarrow$ 6)-linked glucan holding  $\beta$ -D-(1 $\rightarrow$ 3)-side chains (DB of 0.14). This polysaccharide represented an important fraction of the overall *C. albicans*  $\beta$ -glucans ( $46.3 \pm 6.4\%$ ). A very similar, although less abundant (about 15%)  $\beta$ -D-(1 $\rightarrow$ 6)-linked glucan component (DP about 130–140, DB about 0.14) was isolated in the early 1970s by Manners et al. from the cell wall of *Saccharomyces cerevisiae* yeast.<sup>48</sup> Further digestion of *C. albicans* Pool 1 by  $\beta$ -D-(1 $\rightarrow$ 6)-endoglucanase yielded a mixture of glucose, short linear  $\beta$ -D-(1 $\rightarrow$ 6)-linked oligosaccharides (Gn) and 3-branched Gn oligosaccharides, also in agreement with a recent study by Herrero et al.<sup>51</sup> Again, substantially similar findings were reported by Magnelli et al. following  $\beta$ -D-(1 $\rightarrow$ 6)-endoglucanase digestion of  $\beta$ -glucans from *S. cerevisiae*.<sup>26</sup>

Therefore, the patterns associated with GG digestion by  $\beta$ -D-(1 $\rightarrow$ 3)- and  $\beta$ -D-(1 $\rightarrow$ 6)-endoglucanases consistently indicated the presence in *C. albicans* cell wall of  $\beta$ -D-(1 $\rightarrow$ 6)-glucan backbones holding  $\beta$ -D-(1 $\rightarrow$ 3)-side chains. The short size of these branches ( $2.20 \pm 0.02$  units) could result from an extensive zymolyase action on originally longer  $\beta$ -D-(1 $\rightarrow$ 3)-linked glucopyranosyl chains. Since, however,  $\beta$ -D-(1 $\rightarrow$ 3)-side chains of similar short size were also detected by Manners et al.<sup>48</sup> in *S. cerevisiae*  $\beta$ -D-(1 $\rightarrow$ 6)-glucans isolated either by chemical fractionation methods or by selective endoglucanase digestion, it cannot be excluded that the  $\beta$ -D-(1 $\rightarrow$ 6) backbone basically holds short  $\beta$ -D-(1 $\rightarrow$ 3)-side chains. Such a structure may then act as a ‘comb-like’ support on which longer, linear  $\beta$ -D-(1 $\rightarrow$ 3)-linked chains may alternatively form, attach, elongate and detach under the action of dynamic mechanisms mediated by specific enzymes (e.g., 1,3- $\beta$ -glucanosyltransferase<sup>52</sup>). Similar mechanisms have been proposed by Mouyna et al.<sup>53</sup> to take place in *S. cerevisiae*  $\beta$ -glucans and may provide the cell with a powerful means to ensure cell wall integ-

rity and plasticity in response to environmental stimuli or during cell growth.

### 3.2. Structure of $\beta$ -D-(1 $\rightarrow$ 3)-glucan chains in *C. albicans* cell wall

A major question arises on whether the  $\beta$ -D-(1 $\rightarrow$ 6)-backbones described above might (at least in part) also act as side chains of  $\beta$ -D-(1 $\rightarrow$ 3)-linked glucans. In fact, the  $\beta$ -D-(1 $\rightarrow$ 6)-chains isolated in Pool 1 might in turn have been released from GG by  $\beta$ -D-(1 $\rightarrow$ 3)-glucanase digestion of bonds near to  $\beta$ -(1 $\rightarrow$ 3,6)-branch points of  $\beta$ -D-(1 $\rightarrow$ 3)-linked glucans. However, in this case, a portion of short 6-branched  $\beta$ -D-(1 $\rightarrow$ 3)-oligosaccharides should give rise to RT $\alpha$  and RT $\beta$  doublets at (or near)  $\delta$  5.05 and 4.45, typical of the reducing end of  $\beta$ -D-(1 $\rightarrow$ 3)-linked segments. These resonances were actually not detected in the spectrum of Pool 1 nor in that of its  $\beta$ -D-(1 $\rightarrow$ 6)-glucanase digestion products (Figs. 3 and 4), due either to the absence of these oligosaccharides or to their low concentration. These results point to the presence in GG of a large portion of  $\beta$ -D-(1 $\rightarrow$ 3) glucan chains, possessing a very low (if any) degree of branching, also in agreement with a report by Lowman et al.<sup>35</sup> on  $\beta$ -glucans extracted by acids from blastospores or hyphal forms of *C. albicans*. Our study also shows that the fraction of  $\beta$ -D-(1 $\rightarrow$ 3)-linked glucopyranosyl chains account for about 50% of *C. albicans* glucans, as compared to a much higher fraction (about 85%) in *S. cerevisiae*.<sup>54</sup> Beyond its different abundance in the two organisms, it is interesting to note that even in *S. cerevisiae* this component was reported to contain a low percentage (3%) of  $\beta$ -D-(1 $\rightarrow$ 6)-glucosidic inter-chain linkages.

### 3.3. Model for $\beta$ -glucan structure in *C. albicans* cell wall

The overall body of these results is consistent with a structural model in which  $\beta$ -D-(1 $\rightarrow$ 6)-linked glucopyranosyl chains (about 50% of GG content) would act as backbones for branched  $\beta$ -D-(1 $\rightarrow$ 3)-side chains, as depicted in Figure 6. Interestingly, a similar  $\beta$ -glucan structure, in which  $\beta$ -D-(1 $\rightarrow$ 3)-linked glucan is present only in the form of side chains on  $\beta$ -D-(1 $\rightarrow$ 6)-linked molecules has also been reported in *Cryptococcus neoformans*,<sup>55</sup> a pathogenic yeast with a very different cell wall organization as compared to *Candida* and *Saccharomyces*.

The newly identified structure of branched  $\beta$ -D-(1 $\rightarrow$ 6)-linked backbones in *C. albicans* glucan ghosts (Fig. 6) may have some implications on the overall native  $\beta$ -glucan architecture in the cell wall. It is in fact generally proposed that  $\beta$ -D-(1 $\rightarrow$ 3)- and  $\beta$ -D-(1 $\rightarrow$ 6)-glucans have different biological functions, the former providing a structural scaffold to the cell and the latter having a linking and stabilizing role.<sup>26</sup> The structural



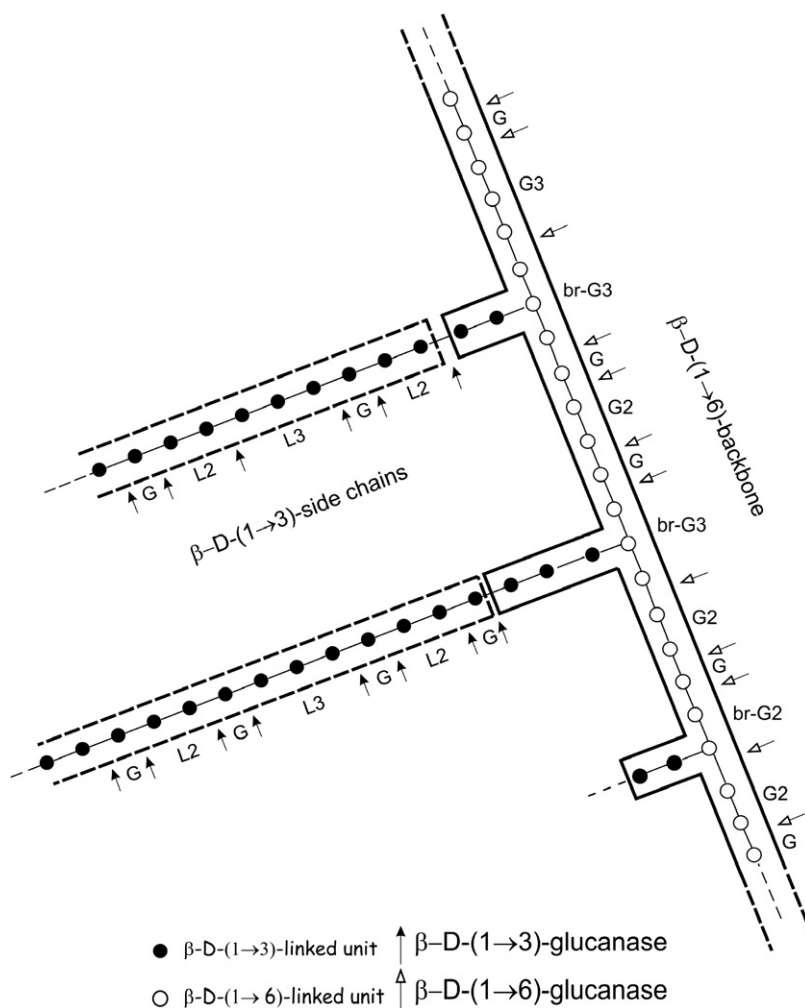


**Figure 6.** Structural model of  $\beta$ -D-(1 $\rightarrow$ 6) glucan holding short  $\beta$ -D-(1 $\rightarrow$ 3)-linked glucopyranosyl side chains (DB, 0.14), isolated (as Pool 1) from *C. albicans* glucan ghost digested by  $\beta$ -D-(1 $\rightarrow$ 3)-endoglucanase (GG-Zym). This glucan component is proposed to act, in the glucan ghost, as a ‘comb-like’ backbone for longer  $\beta$ -D-(1 $\rightarrow$ 3)-linked glucosyl chains (whose  $\beta$ -D-(1 $\rightarrow$ 3)-endoglucanase digestion products mainly consisted of short  $L_n$  and free glucose in Pool 2). G, free glucose;  $L_n$  = linear,  $\beta$ -(1 $\rightarrow$ 3)-linked oligoglucosides of  $n$  units;  $G_n$  = linear,  $\beta$ -(1 $\rightarrow$ 6)-linked oligoglucosides of  $n$  units; br- $G_n$ ,  $\beta$ -D-(1 $\rightarrow$ 3,6)-branched  $G_n$  oligomers. Black arrows point to bonds digested by  $\beta$ -D-(1 $\rightarrow$ 3)-endoglucanase. Empty arrows point to bonds cleaved by  $\beta$ -D-(1 $\rightarrow$ 6)-endoglucanase.

model depicted in Figure 6 strengthens this general view, since the rather rigid, ‘rod-like’ structure of  $\beta$ -D-(1 $\rightarrow$ 6)-chains would at the same time provide anchorage to the cell wall mannoproteins, act as stabilizing cell wall components and serve as backbone for holding long, unbranched  $\beta$ -D-(1 $\rightarrow$ 3)-side chains. The latter could in turn form multiple covalent associations with chitin, as reported by other authors for *S. cerevisiae*<sup>56</sup> or could connect adjacent  $\beta$ -D-(1 $\rightarrow$ 6)-linked chains. Moreover,  $\beta$ -D-(1 $\rightarrow$ 3)-chains could also form a complex network by multiple intermolecular interactions with adjacent homologous chains (e.g., by forming helical structures), so giving rise to a fibrillar network. In this picture, the  $\beta$ -D-(1 $\rightarrow$ 6)-glucan chains described in this study would act as very central molecular components, connecting together all major constituents of the *C. albicans* cell wall. On the other hand, this type of tridimensional polysac-

charide chains architecture would allow the accessibility of linear  $\beta$ -D-(1 $\rightarrow$ 3)-chains to immune host defense attack and may also facilitate the release of these polysaccharides to the blood stream. In general agreement with this, our group has recently demonstrated that mice vaccinated with mannoprotein-deprived, glucan-exposing *C. albicans* cells or with a glycoconjugate, laminarin-based vaccine preparation generated high levels of anti- $\beta$ -glucan antibodies, which preferentially bound to hyphal fungal cells, inhibited their growth in vitro and were highly protective in vivo.<sup>12,15</sup> This observation combines with the detection of anti- $\beta$ -glucan antibodies in normal human sera,<sup>38</sup> to suggest that anti- $\beta$ -glucan immune responses might significantly participate in antifungal protection in the healthy adult and that the relevant antigen can be used to boost the above response.

Finally, our study provides some novel aspects of the characterization of purified, soluble  $\beta$ -glucan fractions of a common fungal pathogen such as *C. albicans*. These may prove useful for the studies of immunomodulatory and antigenic properties of this major fungal cell wall component.

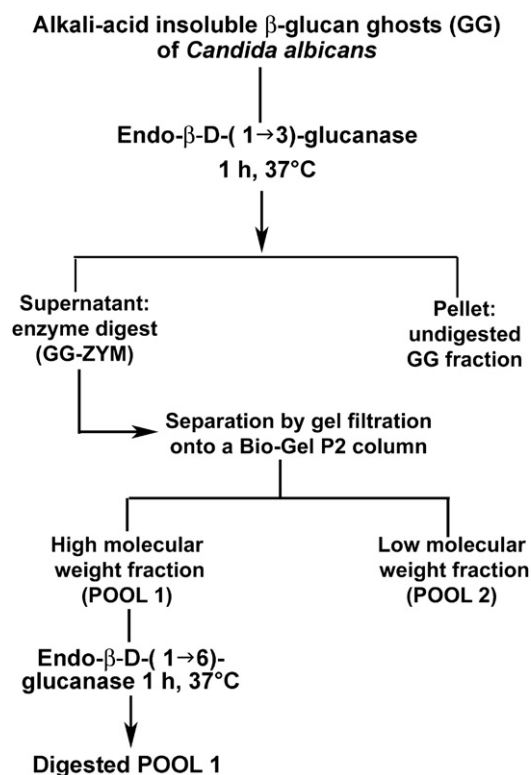
#### 4. Experimental

##### 4.1. $\beta$ -Glucan fractions from *C. albicans* cell wall and standard $\beta$ -glucan compounds

Pure, insoluble GG particles (polysaccharide 95–97% w/w, of which glucose >95%; protein <0.05%) were prepared from cell walls of *C. albicans* by repeated cycles of acid and alkali extraction at 100 °C, essentially as described previously,<sup>21,57</sup> followed by extensive deproteinization (1.5 h at 100 °C) with 2% SDS in 0.1 M Tris–HCl buffer pH 6.8 containing 5 mM EDTA and 100 mM mercaptoethanol. After repeated washing with H<sub>2</sub>O to remove the deproteination mixture, the fraction was lyophilized and stored at 4 °C. To obtain the soluble  $\beta$ -glucan fraction GG-Zym, GG particles (10 mg in phosphate buffer solution (PBS)) were digested for 1 h at 37 °C with a purified endo- $\beta$ -D-(1 $\rightarrow$ 3)-glucanase (Zymolyase 100T; Seikagaku Co., Tokyo, Japan, 200  $\mu$ g). After digestion, GG residues were removed by centrifugation (12,000g, 10 min), the enzyme in the supernatants was heat-inactivated at 100 °C for 5 min and the GG-Zym preparations were stored at –20 °C.

The GG-Zym fraction was separated by gel filtration onto a 75.0 cm height, 1.6 cm diameter bed of Bio-Gel P2 extra-fine resin (nominal exclusion limit 1800 dalton, Bio-Rad Laboratories, Richmond, CA), with 0.02 M PBS as the eluant. Fractions corresponding to carbohydrate peaks were combined together, yielding two distinct subfractions which were, respectively, named Pool 1 (eluted in the column void volume) and Pool 2.

The molecular weight of the Pool 1 fraction was estimated using a Sephacryl S200 resin (Amersham-Pharmacia, Uppsala, Sweden) in a 70 cm height, 1.6 cm diameter-column and with 0.02 M PBS containing 0.1% SDS as the eluant. Retention time of the sample was measured by carbohydrate analysis in the eluate and the molecular mass was estimated by comparison with the elution profile of pustulan. Pool 2 was analyzed onto a Bio-Gel P2 extrafine (Bio-Rad) column (70 cm height, 1.6 cm diameter), previously calibrated with glucose and a series of standard  $\beta$ -D-(1 $\rightarrow$ 3)-gluco-oligosaccharides with a DP ranging from 3 to 7 (L3, L5 and L7), molecular weight 504.4, 828.7 and 1153.0 dalton, respectively (purchased from Seikagaku, Tokyo, Japan). Pool 2 subcomponents were eluted with 0.02 M PBS, and detected by the Dubois' carbohydrate assay.<sup>58</sup> Further digestion of Pool 1 and pustulan (3 mg each in 50 mM acetate buffer, pH 5.5) was obtained by using 20 U of



**Scheme 1.** Preparation of *Candida albicans* insoluble particles (GG), subfractions and glucanase digestion products.

endo- $\beta$ -D-(1 $\rightarrow$ 6)-glucanase for 1 h at 37 °C (Prozyme, San Leandro, CA).

Laminarin from the brown alga *Laminaria digitata* (Sigma Chem. Co., St. Louis, MO), a soluble glucan composed of 20–30  $\beta$ -D-(1 $\rightarrow$ 3)-linked units, with occasional short side chains of  $\beta$ -D-(1 $\rightarrow$ 6)-linked oligoglucosides,<sup>59</sup> and pustulan (Calbiochem, La Jolla, CA) a 20,000 dalton, linear,  $\beta$ -D-(1 $\rightarrow$ 6)-linked glucan from the lichen *Umbilicaria papulosa*, were used as reference standard compounds for NMR analyses. The main steps of the preparation of GG subfractions are summarized in Scheme 1.

##### 4.2. Analytical determinations

Polysaccharides were estimated by the phenol/sulfuric acid method of Dubois et al.,<sup>58</sup> using glucose as standard. Protein concentration was measured by a commercial assay (Bio-Rad), following the manufacturer's instructions.

##### 4.3. <sup>1</sup>H and <sup>13</sup>C NMR spectroscopy

NMR experiments were carried out on Bruker AVANCE spectrometers (Karlsruhe, Germany) operating at 400 or 700 MHz for <sup>1</sup>H and at 100 or 175 MHz for <sup>13</sup>C. Chemical shifts were referenced internally to

sodium 3-(trimethylsilyl)-propionate-2,2,3,3- $d_4$  (TSP,  $\delta$ , 0.00) for  $^1\text{H}$  signals and to  $\text{Me}_2\text{SO}-d_6$  ( $\delta$ , 39.50) for  $^{13}\text{C}$ . Before NMR analyses, the glucan fractions were subjected to three cycles of solubilization in 99.9%  $\text{D}_2\text{O}$  (Calbiochem Isotopes), each followed by freeze-drying, to convert OH into OD groups.

For  $^1\text{H}$  NMR spectra of samples in  $\text{D}_2\text{O}$ , 32 K complex data points were acquired (acquisition time (AQ) = 2.04 s), and 128 free induction decay signals (FIDs) were averaged with a  $60^\circ$  observe pulse, preceded by a 5.0 s pre-saturation pulse, for residual HDO signal suppression.

For  $^{13}\text{C}$  experiments, 64 K complex data points were acquired and 4000 scans were averaged with a  $30^\circ$  observe pulse, AQ = 1.4 s and repetition delay 5 s.

Two-dimensional magnitude correlation spectroscopy (COSY) and hetero-nuclear single quantum correlation spectroscopy (HSQC) were performed for unambiguous assignment of  $^1\text{H}$  and  $^{13}\text{C}$  resonances. For COSY experiments,  $1024 (t_2) \times 256 (t_1)$  complex data points were acquired, and 32 scans were averaged for each FID with a relaxation delay of 2.5 s. For HSQC,  $2048 (t_2) \times 256 (t_1)$  complex data points were acquired with a relaxation delay of 2.5 s, and 64 scans were averaged for each FID.

For peak assignment and relative quantification of all individual  $^1\text{H}$  NMR signals in C1 position (H1) of different glucopyranosyl units under conditions preventing glucan aggregation, the samples were dissolved in a mixed solution of 6:1 (v/v)  $\text{Me}_2\text{SO}-d_6$ – $\text{D}_2\text{O}$  at  $80^\circ\text{C}$ <sup>28</sup> and the spectra were taken (32 K complex data points acquisition, 128 FIDs averaging, with a  $30^\circ$  observe pulse, AQ = 4.05 s and 5.0 s pulse delay). The FIDs were zero-filled to 64 K complex data points and the spectra were baseline corrected (in the frequency domain) for peak area integration. The pulse sequence adopted for  $^1\text{H}$  spectral acquisition allowed reliable quantification (within  $\pm 5\%$ ) of peak area ratios in the spectra of both short and long glucopyranosyl chains in  $\text{Me}_2\text{SO}-d_6$ – $\text{D}_2\text{O}$ , as already reported by Kim et al.<sup>28</sup> and verified in our laboratory, by using a fixed flip angle ( $30^\circ$ ) and different pulse delays ranging from 5 to 50 s.

### Acknowledgements

This work was partially supported by a special Project of Italian Ministry of Health, N. ISS/0AD/F. We are indebted to Mr. Massimiliano Ferrara for technical assistance.

### References

- Stone, B. A.; Clark, A. E. *Chemistry and Biology of (1-3)- $\beta$ -Glucans*; La Trobe University Press: Bundoora, 1992; pp 1–116.
- Masuoka, J. *Clin. Microbiol. Rev.* **2004**, *17*, 281–310.
- Bohn, J. A.; BeMiller, J. N. *Carbohydr. Polym.* **1995**, *28*, 3–14.
- Cassone, A. *Drugs Exp. Clin. Res.* **1986**, *12*, 635–643.
- Brown, G. D.; Gordon, S. *Immunity* **2003**, *19*, 311–315.
- Chattaway, F. W.; Holmes, M. R.; Barlow, A. J. *J. Gen. Microbiol.* **1968**, *51*, 367–376.
- Cassone, A.; Torosantucci, A. In *Candida albicans*; Prasad, R., Ed.; Springer: Berlin, Heidelberg, 1991; pp 89–107.
- Klis, F. M.; de Groot, P.; Hellingwerf, K. *Med. Mycol.* **2001**, *39*, 1–8.
- Ohno, N.; Uchiyama, M.; Tsuzuki, A.; Tokunaka, K.; Miura, N. N.; Adachi, Y.; Aizawa, M. W.; Tamura, H.; Tanaka, S.; Yadomae, T. *Carbohydr. Res.* **1999**, *316*, 161–172.
- Sato, T.; Iwabuchi, K.; Nagaoka, I.; Adachi, Y.; Ohno, N.; Tamura, H.; Seyama, K.; Fukuchi, Y.; Nakayama, H.; Yoshizaki, F.; Takamori, K.; Ogawa, H. *J. Leukocyte Biol.* **2006**, *80*, 204–211.
- Georgopapadakou, N. H.; Tkacz, J. S. *Trends Microbiol.* **1995**, *3*, 98–104.
- Torosantucci, A.; Bromuro, C.; Chiani, P.; De Bernardis, F.; Berti, F.; Galli, C.; Norelli, F.; Bellucci, C.; Polonelli, L.; Costantino, P.; Rappuoli, R.; Cassone, A. *J. Exp. Med.* **2005**, *202*, 597–606.
- Denning, D. W. *Lancet* **2003**, *362*, 1142–1151.
- Magliani, W.; Conti, S.; Salati, A.; Arseni, S.; Ravanetti, L.; Frazzi, R.; Polonelli, L. *Curr. Med. Chem.* **2004**, *11*, 1793–1800.
- Bromuro, C.; Torosantucci, A.; Chiani, P.; Conti, S.; Polonelli, L.; Cassone, A. *Infect. Immun.* **2002**, *70*, 5462–5470.
- Uchiyama, M.; Ohno, N.; Miura, N. N.; Adachi, Y.; Tamura, H.; Tanaka, S.; Yadomae, T. *Biol. Pharm. Bull.* **2000**, *23*, 672–676.
- Adachi, Y.; Ohno, N.; Yadomae, T. *Biol. Pharm. Bull.* **1994**, *17*, 1508–1512.
- Gorin, P. A. J. *Adv. Carbohydr. Chem. Biochem.* **1981**, *38*, 13–39.
- Egan, W. *Dev. Biol. (Basel)* **2000**, *103*, 3–9.
- Urhin, D.; Brisson, J. R. In *NMR in Microbiology Theory and Applications*; Barbotin, J., Portais, J., Eds.; Horizon Scientific Press: Wymondham, 2000; pp 165–190.
- Scaringi, L.; Marconi, P.; Boccanera, M.; Tissi, L.; Bistoni, F.; Cassone, A. *J. Gen. Microbiol.* **1988**, *134*, 1265–1274.
- Bassieux, D.; Gagnaire, D.; Vignon, M. *Carbohydr. Res.* **1977**, *56*, 19–33.
- Petersen, B. O.; Krah, M.; Duus, J. O.; Thomsen, K. K. *Eur. J. Biochem.* **2000**, *267*, 361–369.
- Kulminkaya, A. A.; Thomsen, K. K.; Shabalin, K. A.; Sidorenko, I. A.; Eneyskaya, E. V.; Savel'ev, A. N.; Neustroev, K. N. *Eur. J. Biochem.* **2001**, *268*, 6123–6131.
- Lo, V. M.; Hahn, M. G.; Hong, N.; Ogawa, T.; van Halbeck, H. *Carbohydr. Res.* **1993**, *245*, 333–345.
- Magnelli, P.; Cipollo, J. F.; Abeijon, C. *Anal. Biochem.* **2002**, *301*, 136–150.
- Wilker, W.; Leibfritz, R.; Kerssebaum, R.; Bermel, W. *Magn. Reson. Chem.* **1993**, *31*, 287–292.
- Kim, Y. T.; Kim, E. H.; Cheong, C.; Williams, D. L.; Kim, C. W.; Lim, S. T. *Carbohydr. Res.* **2000**, *328*, 331–341.
- Gopal, P. K.; Shepherd, M. G.; Sullivans, P. A. *J. Gen. Microbiol.* **1984**, *130*, 3295–3301.
- Hartland, R. P.; Emerson, G. W.; Sullivan, P. A. *Proc. Biol. Sci.* **1991**, *247*, 155–160.

31. Ensley, H. E.; Tobias, B.; Petrus, H. A.; McNamee, R. B.; Jones, E. L.; Browder, I. W.; Williams, D. L. *Carbohydr. Res.* **1994**, 258, 307–311.
32. Kollar, R.; Reinhold, B. B.; Petr  kova, E.; Yeh, H. J. C.; Ashwell, G.; Drgonova, J.; Kapteyn, J. C.; Klis, F. M.; Cabib, E. *J. Biol. Chem.* **1997**, 272, 17762–17775.
33. Carbonero, E. R.; Sassaki, G. L.; Stuelp, P. M.; Gorin, P. A.; Woranocivz-Barriera, S. M.; Iacomini, M. *FEMS Microbiol. Lett.* **2001**, 194, 65–69.
34. Miura, N. N.; Adachi, Y.; Yadomae, T.; Tamura, H.; Tanaka, S.; Ohno, N. *Microbiol. Immunol.* **2003**, 47, 173–182.
35. Lowman, D. W.; Ferguson, D. A.; Williams, D. L. *Carbohydr. Res.* **2003**, 338, 1491–1496.
36. Williams, D. L.; McNamee, R. B.; Jones, E. L.; Pretus, H. A.; Ensley, H. E.; Browder, W.; Di Luzio, N. R. *Carbohydr. Res.* **1991**, 219, 293–313.
37. Keller, R. G.; Pfrommer, G. S.; Kozel, T. R. *Infect. Immun.* **1994**, 62, 215–220.
38. Goldman, R. C.; Frost, D. J.; Capobianco, J. O.; Kadam, S.; Rasmussen, R. R.; Abad-Zapatero, C. *Infect. Agents Dis.* **1995**, 4, 228–247.
39. Yadomae, T.; Ohno, N. *Rec. Devel. Chem. Pharm. Sci.* **1996**, 1, 23–33.
40. Tokunaka, K.; Ohno, N.; Adachi, Y.; Tanaka, S.; Tamura, H.; Yadomae, T. *Int. J. Immunopharmacol.* **2000**, 22, 383–394.
41. Nagi, N.; Ohno, N.; Adachi, Y.; Aketagawa, J.; Tamura, H.; Shibata, Y.; Tanaka, S.; Yadomae, T. *Biol. Pharm. Bull.* **1993**, 16, 822–828.
42. Ohno, N.; Asada, N.; Adachi, Y.; Yadomae, T. *Biol. Pharm. Bull.* **1995**, 18, 126–133.
43. Ohno, N.; Hashimoto, T.; Adachi, Y.; Yadomae, T. *Immunol. Lett.* **1996**, 53, 157–163.
44. Rinaudo, M.; Vincendon, M. *Carbohydr. Polym.* **1982**, 2, 135–144.
45. Iino, K.; Ohno, N.; Suzuki, I.; Miyazaki, T.; Yadomae, T.; Oikawa, S.; Sato, S. *Carbohydr. Res.* **1982**, 14, 111–119.
46. Ohno, N.; Suzuki, I.; Yadomae, T. *Chem. Pharm. Bull. (Tokyo)* **1986**, 34, 1362–1365.
47. Saito, K.; Nishijima, M.; Ohno, N.; Yadomae, T.; Miyazaki, T. *Chem. Pharm. Bull. (Tokyo)* **1992**, 40, 261–263.
48. Manners, D. J.; Masson, A. J.; Patterson, J. C.; Bjorndal, H.; Lindberg, B. *Biochem. J.* **1973**, 135, 31–36.
49. Gale, E. F.; Ingram, J.; Kerridge, D.; Notario, V.; Wayman, F. J. *Gen. Microbiol.* **1980**, 117, 383–391.
50. Ohno, N.; Miura, N. N.; Nakajima, M.; Yadomae, T. *Biol. Pharm. Bull.* **2000**, 23, 866–872.
51. Herrero, A. B.; Magnelli, P.; Mansour, M. K.; Levitz, S. M.; Bussey, H.; Abeijon, C. *Eukaryot. Cell.* **2004**, 3, 1423–1432.
52. Ram, A. F.; Kaptein, J. C.; Montijn, R. C.; Caro, L. H. P.; Douwes, J. E.; Baginsky, W.; Manzur, P.; Van den Ende, H.; Klis, F. M. *J. Bacteriol.* **1998**, 180, 1418–1424.
53. Mouyna, I.; Fontaine, T.; Vai, M.; Monod, M.; Fonzi, W. A.; Diaquin, M.; Popolo, L.; Hartland, R. P.; Latge, J. P. *J. Biol. Chem.* **2000**, 275, 14882–14889.
54. Manners, D. J.; Masson, A. J.; Patterson, J. C. *Biochem. J.* **1973**, 135, 19–30.
55. James, P. G.; Cherniak, R.; Jones, R. G.; Stortz, C. A.; Reiss, E. *Carbohydr. Res.* **1990**, 198, 23–38.
56. Kollar, R.; Petr  kova, E.; Ashwell, G.; Robbins, P. W.; Cabib, E. *J. Biol. Chem.* **1995**, 270, 1170–1178.
57. Torosantucci, A.; Chiani, P.; Cassone, A. *J. Leukocyte Biol.* **2000**, 68, 923–932.
58. Dubois, M.; Gilles, K.; Hamilton, J. K.; Rebers, P. A.; Smith, F. *Anal. Chem.* **1956**, 28, 350–356.
59. Read, S. M.; Currie, G.; Bacic, A. *Carbohydr. Res.* **1996**, 281, 187–201.